

# Green's Function for Layered Lossy Media with Special Application to Microstrip Antennas

LUC BEYNE AND DANIEL DE ZUTTER

**Abstract**—Suitable Green's dyadics for the fields generated by a surface current density in a plane parallel to the interface of a layered isotropic structure are determined. Special care is taken to ensure that the Green's function can still be calculated in the source region by circumventing the numerical problems by analytical procedures. As it is our purpose to use the obtained Green's function in order to calculate the power deposition from a microstrip antenna inside a layered biological tissue, the media involved can be highly lossy. An analytical method is developed to avoid numerical problems arising from the exponential decay of the fields due to these losses.

## I. INTRODUCTION

THE PROBLEM OF electromagnetic propagation in stratified media, both isotropic and anisotropic, has been studied extensively in the past. A short review of relevant papers can be found in the introductions of three recent papers on the same topic [1]–[3]. The present paper focuses on the calculation of a suitable Green's function for the fields generated by a surface current density in a plane parallel to the interface of a layered isotropic structure. This situation is of great practical importance for the calculation of microstrip antennas buried in a stratified medium. Special care is taken to ensure that the Green's function can still be calculated in the source region by circumventing the numerical problems by suitable analytical procedures. As it is our purpose to use the Green's function in order to calculate the power deposition inside a layered biological tissue, the media involved can be highly lossy. An analytical method is developed to avoid numerical problems arising from the exponential decay of the fields due to these losses. As in [4] and [5], our full-wave analysis starts from the spatial Fourier domain.

In contrast to our approach, the FFT method proposed in [2] is not suited for calculations if observation point and source point coincide. This is essential if the Green's function must serve as the basis for solving an integral equation for the current on a microstrip patch. The calculations presented in [1] did not lead to a formulation

Manuscript received August 19, 1987; revised November 24, 1987. This work was supported by the National Fund for Scientific Research of Belgium.

L. Beyne was with the Laboratory of Electromagnetism and Acoustics, University of Ghent, Belgium. He is now with Alcatel Bell Telephone, Antwerp, Belgium.

D. De Zutter is with the Laboratory of Electromagnetism and Acoustics, University of Ghent, 9000 Ghent, Belgium.

IEEE Log Number 8819967.

suitable for solving microstrip antenna problems, as indicated in the introduction of [6], where a mixed-potential integral equation is stated to be superior. The approach based on a vector potential and a scalar potential is also adopted in [3] to compare quasi-static results with the results from a full-wave analysis for a horizontal dipole on a microstrip. Although our approach is basically similar to the one proposed in [1], we show that additional analytical efforts enable us to circumvent difficulties with the convergence of the inverse Fourier–Bessel integrals in the plane of the source. This leads to a correct evaluation of the Green's function everywhere and paves the way to solving the integral equation for a microstrip antenna in a lossy stratified medium. The solution of this problem for a microstrip applicator radiating into a layered biological medium is proposed elsewhere [7].

## II. GEOMETRY AND GENERAL FORMULATION OF THE PROBLEM

We restrict our attention to the layered medium shown on Fig. 1. The half-space  $z > 0$  is bounded by a perfectly conducting plane at  $z = 0$  and the excitation is a surface current  $\mathbf{J}_S$  at the first interface  $z = d_1$ . The layers are lossy; hence the  $\epsilon$ 's can take complex values. The analysis can easily be extended to other configurations. The sinusoidal time dependence  $\exp(j\omega t)$  is suppressed throughout the text. From the linearity of the problem it follows that the  $\mathbf{E}$  and  $\mathbf{H}$  fields everywhere in space depend upon the surface current density  $\mathbf{J}_S$  as follows:

$$\begin{aligned} \mathbf{E}(\mathbf{r}) &= \iint \bar{\bar{G}}_e(\mathbf{r}|\mathbf{r}') \cdot \mathbf{J}_S(\mathbf{r}') dS' \\ \mathbf{H}(\mathbf{r}) &= \iint \bar{\bar{G}}_h(\mathbf{r}|\mathbf{r}') \cdot \mathbf{J}_S(\mathbf{r}') dS'. \end{aligned} \quad (1)$$

Here  $\bar{\bar{G}}_e$  and  $\bar{\bar{G}}_h$  represent the electric and magnetic Green's dyadic. The point with position vector  $\mathbf{r} = \mathbf{r}_t + z\mathbf{u}_z$  is an arbitrary observation point. The position vector  $\mathbf{r}' = \mathbf{r}'_t + d_1\mathbf{u}_z$  refers to a variable integration point on the surface of the metal patch (see Fig. 1). As the configuration under consideration is homogeneous in the transversal ( $x, y$ ) directions, both dyadics satisfy the property:

$$\bar{\bar{G}}(\mathbf{r}|\mathbf{r}') = \bar{\bar{G}}(\mathbf{r} - \mathbf{r}'|d_1\mathbf{u}_z). \quad (2)$$

The fields satisfy Maxwell's equations in each layer of the

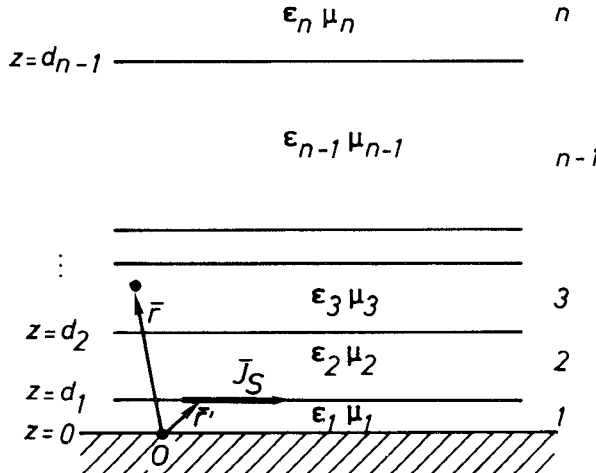


Fig. 1. Surface current density radiating into a layered medium.

medium:

$$\begin{aligned} \operatorname{curl} \mathbf{E} &= -j\omega\mu\mathbf{H} \\ \operatorname{curl} \mathbf{H} &= j\omega\epsilon\mathbf{E} \\ \operatorname{div} \mathbf{E} &= 0 \\ \operatorname{div} \mathbf{H} &= 0. \end{aligned} \quad (3)$$

Both  $\epsilon$  and  $\mu$  can be complex.

### III. SOLUTION IN THE FOURIER DOMAIN

As a first step we introduce the Fourier transformation of all fields with respect to the transversal coordinates. The vector  $\mathbf{k} = k_x \mathbf{u}_x + k_y \mathbf{u}_y$  represents the position vector in Fourier space. The Fourier transformation and its inverse are defined as follows:

$$\begin{aligned} f(z, \mathbf{k}) &= \int_{-\infty}^{+\infty} \int_{-\infty}^{+\infty} f(\mathbf{r}) \exp(j\mathbf{k} \cdot \mathbf{r}) dx dy \\ f(\mathbf{r}) &= (1/2\pi)^2 \int_{-\infty}^{+\infty} \int_{-\infty}^{+\infty} f(z, \mathbf{k}) \\ &\quad \cdot \exp(-j\mathbf{k} \cdot \mathbf{r}) dk_x dk_y. \end{aligned} \quad (4)$$

As there is no danger for confusion, we have not introduced a special symbol to indicate the Fourier transformation. A function and its transformation are only distinguished by their arguments.

It is easy to see that the transformed fields satisfy

$$\begin{aligned} \frac{d^2 \mathbf{E}}{dz^2} - \Gamma^2 \mathbf{E} &= 0 \\ \frac{d^2 \mathbf{H}}{dz^2} - \Gamma^2 \mathbf{H} &= 0 \end{aligned} \quad (5)$$

where  $\Gamma^2 = k_x^2 + k_y^2 - k^2$ . In each layer the wavenumber  $k$  is given by  $k_0 N$ , where  $k_0 = \omega/c$  is the free-space wavenumber and  $N = (\epsilon_r \mu_r)^{1/2}$  is the complex refractive index of that layer.  $\Gamma$  itself is defined as the root of  $\Gamma^2$  with nonnegative real or imaginary part. The solution of (5) is given by

$$\begin{aligned} \mathbf{E}(z, \mathbf{k}) &= \mathbf{A} \exp(-\Gamma z) + \mathbf{B} \exp(\Gamma z) \\ \mathbf{H}(z, \mathbf{k}) &= \mathbf{K} \exp(-\Gamma z) + \mathbf{L} \exp(\Gamma z). \end{aligned} \quad (6)$$

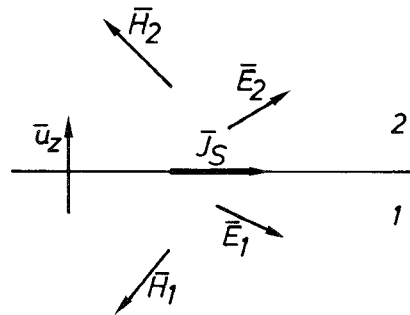


Fig. 2. Boundary conditions at the interface of two media.

The vectors  $\mathbf{K}$  and  $\mathbf{L}$  are not independent of  $\mathbf{A}$  and  $\mathbf{B}$ . The relation between them will be established below.

As a second and essential step, we introduce the projection of every vector on three orthogonal directions. An arbitrary vector  $\mathbf{W}$  is characterized by the three numbers  $W_z$ ,  $W'$ , and  $W''$  as follows:

$$\mathbf{W} = W_z \mathbf{u}_z + [W' \mathbf{k} + W'' (\mathbf{u}_z \times \mathbf{k})] / (k_x^2 + k_y^2). \quad (7)$$

It is clear that  $E'$ ,  $E''$ ,  $E_z$ ,  $H'$ ,  $H''$ , and  $H_z$  are of the form (6) but with the vectors replaced by scalars. With the notation introduced above, the divergence equations in (3) reduce to  $dE_z/dz = jE'$  and to  $dH_z/dz = jH'$ . The rotor equations projected on the  $z$  axis yield the relations  $E'' = \omega\mu H_z$  and  $H'' = -\omega\epsilon E_z$ . Taking the above results and considerations into account, we finally arrive at the following representation of the fields in each layer:

$$E'(z, \mathbf{k}) = A' \exp(-\Gamma z) + B' \exp(\Gamma z)$$

$$H''(z, \mathbf{k}) = (j\omega\epsilon/\Gamma) [A' \exp(-\Gamma z) - B' \exp(\Gamma z)]$$

$$E_z(z, \mathbf{k}) = (-j/\Gamma) [A' \exp(-\Gamma z) - B' \exp(\Gamma z)] \quad (8)$$

and

$$E''(z, \mathbf{k}) = A'' \exp(-\Gamma z) + B'' \exp(\Gamma z)$$

$$H'(z, \mathbf{k}) = [\Gamma/(-j\omega\mu)] [A'' \exp(-\Gamma z) - B'' \exp(\Gamma z)]$$

$$H_z(z, \mathbf{k}) = (1/\omega\mu) [A'' \exp(-\Gamma z) + B'' \exp(\Gamma z)]. \quad (9)$$

As shown by (8) and (9), this representation of the fields falls apart into two sets of decoupled equations: one set for  $E'$ ,  $H''$ , and  $E_z$  and a second set for  $E''$ ,  $H'$ , and  $H_z$ . The first set is a TM mode as the  $z$  component of the magnetic field is zero. The second set is a TE mode. The couples  $(E', H'')$  and  $(E'', H')$  behave as voltage and current across a transmission line. The constants  $A'$ ,  $B'$  and  $A''$ ,  $B''$  must be determined by applying the boundary conditions between the layers of the medium. The continuity of the tangential electric field between layer 1 and layer 2, (see Fig. 2) leads to

$$E'_1 - E'_2 = 0$$

$$E''_1 - E''_2 = 0. \quad (10)$$

The tangential magnetic field is also continuous across the boundary of two layers except for  $z = d_1$ , where the Fourier-transformed surface current density  $J_s$  is present (see Fig. 2). In that case the appropriate boundary condi-

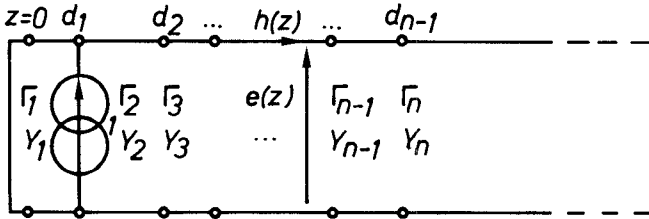


Fig. 3. Transmission line equivalent with unit current source.

tion is

$$\begin{aligned} H'_1 - H'_2 &= -J'_S \\ H''_1 - H''_2 &= +J''_S. \end{aligned} \quad (11)$$

Additional boundary conditions are given by the fact that  $E'$  and  $E''$  are zero at the perfectly conducting ground plane, i.e., for  $z = 0$ ; hence  $A'_1 + B'_1 = 0$  and  $A''_1 + B''_1 = 0$ . Finally, in the uppermost layer, only outgoing waves can exist. This implies  $B'_n = 0$  and  $B''_n = 0$ .

When we take all boundary conditions into account, the final form taken by the fields can be expressed very concisely by introducing the following functions:

$$\begin{aligned} e'(z, \mathbf{k}) &= -E'(z, \mathbf{k})/J'_S(\mathbf{k}) \\ e''(z, \mathbf{k}) &= +E''(z, \mathbf{k})/J''_S(\mathbf{k}) \\ h'(z, \mathbf{k}) &= -H''(z, \mathbf{k})/J'_S(\mathbf{k}) \\ h''(z, \mathbf{k}) &= +H'(z, \mathbf{k})/J''_S(\mathbf{k}). \end{aligned} \quad (12)$$

In both cases,  $e$  and  $h$  in each layer can be written as

$$\begin{aligned} e(z, \mathbf{k}) &= \alpha(\mathbf{k}) \exp(-\Gamma z) + \beta(\mathbf{k}) \exp(\Gamma z) \\ h(z, \mathbf{k}) &= Y(\mathbf{k}) [\alpha(\mathbf{k}) \exp(-\Gamma z) - \beta(\mathbf{k}) \exp(\Gamma z)]. \end{aligned} \quad (13)$$

The  $e$  and  $h$  functions can be determined through the solution of a single transmission line problem. This transmission line equivalent is shown in Fig. 3. The source is a unit current source located at  $z = d_1$ . In the single-prime case, the characteristic admittance  $Y = Y' = j\omega\epsilon/\Gamma$ . In the double-prime case  $Y = Y'' = -\Gamma/j\omega\mu$ . The transmission line formalism to study stratified media was extensively used in the past [8]–[11]. The determination of the  $\alpha$ 's and  $\beta$ 's in each layer seems straightforward. However, due to the presence of increasing and decaying exponentials, the numerical problem is rather heavy and some analytical preprocessing must take place in order to develop a numerically stable procedure, especially in the presence of highly lossy materials, as in the case of biological tissues.

At the first interface ( $z = d_1$ ), the presence of the surface current density leads to the following relationship:

$$(1/2) \begin{vmatrix} (1+u) \exp(\Gamma_1 - \Gamma_2) d_1 & (1-u) \exp(\Gamma_1 + \Gamma_2) d_1 \\ (1-u) \exp(-\Gamma_1 + \Gamma_2) d_1 & (1+u) \exp(\Gamma_2 - \Gamma_1) d_1 \end{vmatrix}$$

$$\cdot \begin{vmatrix} \alpha_2 \\ \beta_2 \end{vmatrix} + \begin{vmatrix} (-1/2Y_1) \exp(\Gamma_1 d_1) \\ (1/2Y_1) \exp(-\Gamma_1 d_1) \end{vmatrix} = \begin{vmatrix} \alpha_1 \\ \beta_1 \end{vmatrix} \quad (14)$$

where  $u = Y_2/Y_1$ . For the other interfaces ( $z = d_j$ ,  $j =$

$2, \dots, n-1$ ) we have

$$(1/2) \begin{vmatrix} (1+v) \exp(\Gamma_j - \Gamma_{j+1}) d_j & (1-v) \exp(\Gamma_{j+1} + \Gamma_j) d_j \\ (1-v) \exp(-\Gamma_j + \Gamma_{j+1}) d_j & (1+v) \exp(\Gamma_{j+1} - \Gamma_j) d_j \end{vmatrix} \cdot \begin{vmatrix} \alpha_{j+1} \\ \beta_{j+1} \end{vmatrix} = \begin{vmatrix} \alpha_j \\ \beta_j \end{vmatrix} \quad (15)$$

where  $v = Y_{j+1}/Y_j$ . A modified form of the matrices in (14) and (15) and their inverses forms the basis of a suitable algorithm for the calculation of the  $\alpha$ 's and  $\beta$ 's. We refer the reader to the Appendix for the final results and a proof of the numerical stability of the proposed method.

#### IV. INVERSE FOURIER TRANSFORMATION AND FOURIER–BESSEL INTEGRALS

##### A. General Formulation

The dyadics  $\bar{\bar{G}}_e(\mathbf{r}|\mathbf{r}')$  and  $\bar{\bar{G}}_h(\mathbf{r}|\mathbf{r}')$  both satisfy the property expressed by (2). If we represent the Fourier transformation of  $\bar{\bar{G}}_e(\mathbf{r}|\mathbf{r}' = d_1 \mathbf{u}_z)$  and  $\bar{\bar{G}}_h(\mathbf{r}|\mathbf{r}' = d_1 \mathbf{u}_z)$ , i.e., for  $\mathbf{r}' = 0$  by, respectively,  $\bar{\bar{G}}_e(z, \mathbf{k})$  and  $\bar{\bar{G}}_h(z, \mathbf{k})$ , the convolutions in (1) together with the property (2) lead to the following result in the Fourier domain:

$$\begin{aligned} \mathbf{E}(z, \mathbf{k}) &= \bar{\bar{G}}_e(z, \mathbf{k}) \cdot \mathbf{J}_S(\mathbf{k}) \\ \mathbf{H}(z, \mathbf{k}) &= \bar{\bar{G}}_h(z, \mathbf{k}) \cdot \mathbf{J}_S(\mathbf{k}). \end{aligned} \quad (16)$$

We introduce the polar coordinates  $\lambda$  and  $\phi$  in the  $(k_x, k_y)$  plane:  $k_x = \lambda \cos \phi$  and  $k_y = \lambda \sin \phi$ . If we take a close look at  $e$  and  $h$ , we see that they depend only upon  $\lambda$  and not on  $\phi$ . We now turn to the  $x$ ,  $y$ , and  $z$  components of  $\mathbf{E}(z, \mathbf{k})$  and  $\mathbf{H}(z, \mathbf{k})$ , taking into account the projection equation (7). Starting from (8), (9), and (12),  $\mathbf{E}$  and  $\mathbf{H}$  can be expressed in terms of the  $x$  and  $y$  components of  $\mathbf{J}_S(\mathbf{k})$ . This leads to the following final form for the Green's dyadics:

$$\begin{aligned} \bar{\bar{G}}_e(z, \mathbf{k}) &= \begin{vmatrix} -e' \cos^2 \phi + e'' \sin^2 \phi & -(e' + e'') \cos \phi \sin \phi \\ -(e' + e'') \cos \phi \sin \phi & -e' \sin^2 \phi + e'' \cos^2 \phi \\ (1/\omega\epsilon) h' \lambda \cos \phi & (1/\omega\epsilon) h' \lambda \sin \phi \end{vmatrix} \\ &= \begin{vmatrix} -h'' - h' & h'' \cos^2 \phi + h' \sin^2 \phi \\ -h'' \sin^2 \phi - h' \cos^2 \phi & (h'' - h') \cos \phi \sin \phi \\ -(1/\omega\mu) e'' \lambda \sin \phi & (1/\omega\mu) e'' \lambda \cos \phi \end{vmatrix} \end{aligned} \quad (17)$$

and

$$\begin{aligned} \bar{\bar{G}}_h(z, \mathbf{k}) &= \begin{vmatrix} -(h'' - h') \cos \phi \sin \phi & h'' \cos^2 \phi + h' \sin^2 \phi \\ -h'' \sin^2 \phi - h' \cos^2 \phi & (h'' - h') \cos \phi \sin \phi \\ -(1/\omega\mu) e'' \lambda \sin \phi & (1/\omega\mu) e'' \lambda \cos \phi \end{vmatrix} \end{aligned} \quad (18)$$

Our final goal is to calculate the inverse Fourier transformation of the above dyadics. For this purpose we introduce the polar coordinates  $\rho$  and  $\theta$  in the  $(x, y)$  plane:  $x = \rho \cos \theta$  and  $y = \rho \sin \theta$ . If we also introduce  $\psi = \phi - \theta$ ,

the inverse Fourier transformation in (4) takes the form

$$f(\rho, \theta, z) = (1/2\pi)^2 \int_0^\infty \int_0^{2\pi} f(z, \lambda, \phi) e^{-j\lambda\rho \cos\psi} \lambda d\lambda d\phi. \quad (19)$$

If  $f(z, \lambda, \phi)$  can be written as

$$f(z, \lambda, \phi) = \sum_{m=0}^{\infty} c_m(z, \lambda, \theta) \cos m\psi + \sum_{m=0}^{\infty} s_m(z, \lambda, \theta) \sin m\psi \quad (20)$$

then  $f(\rho, \theta, z)$  becomes

$$f(\rho, \theta, z) = (1/2\pi) \sum_{m=0}^{\infty} (-j)^m \cdot \int_0^\infty c_m(z, \lambda, \theta) J_m(\lambda\rho) \lambda d\lambda. \quad (21)$$

To obtain this result we used the following integrals:

$$\int_0^{2\pi} \cos m\theta e^{-jz \cos\theta} d\theta = 2\pi(-j)^m J_m(z) \\ \int_0^{2\pi} \sin m\theta e^{-jz \cos\theta} d\theta = 0. \quad (22)$$

We now apply the results given by (20) and (21) to find the inverse Fourier transformation of the dyadics in (17) and (18). We remark that all elements of  $\bar{\bar{G}}_e$  and  $\bar{\bar{G}}_h$  can be written in the form (20) but with  $m$  restricted to 0, 1, or 2. Application of (21) gives the following final result:

$$\bar{\bar{G}}_e(\mathbf{r}|0) = \begin{vmatrix} W_0^e - W_2^e \cos 2\theta & -W_2^e \sin 2\theta \\ -W_2^e \sin 2\theta & W_0^e + W_2^e \cos 2\theta \\ W_1^e \cos \theta & W_1^e \sin \theta \end{vmatrix} \\ \bar{\bar{G}}_h(\mathbf{r}|0) = \begin{vmatrix} -W_2^h \sin 2\theta & W_0^h + W_2^h \cos 2\theta \\ -W_0^h + W_2^h \cos 2\theta & W_2^h \sin 2\theta \\ -W_1^h \sin \theta & W_1^h \cos \theta \end{vmatrix} \quad (23)$$

The argument  $(\mathbf{r}|0)$  of the dyadics indicates that the result is valid for a point source located at  $\mathbf{r}' = d_1 \mathbf{u}_z$ , hence for  $x' = y' = 0$ . The property (2) allows us to find  $\bar{\bar{G}}_e$  and  $\bar{\bar{G}}_h$  for arbitrary  $\mathbf{r}$  and  $\mathbf{r}'$ . The  $W_i$  in (23) are

$$W_i(\rho, z) = (1/2\pi) \int_0^\infty w_i(z, \lambda) J_i(\lambda\rho) \lambda d\lambda \quad (24)$$

with the following values for the  $w_i$ :

$$w_0^e = (-e' + e'')/2 \quad w_0^h = (h' + h'')/2 \\ w_1^e = h'\lambda/(j\omega\epsilon) \quad w_1^h = e''\lambda/(j\omega\mu) \\ w_2^e = -(e' + e'')/2 \quad w_2^h = (h' - h'')/2. \quad (25)$$

To calculate  $W_i$  it is important to know the kind of singularities that occur in the complex  $\lambda$  plane. Although a strict proof can be given, we only state the final result, which is a familiar one [12]. The only branch cut is the branch cut originating from  $\Gamma_n$  of the uppermost layer of the medium. As we only treat the case of a layered

TABLE I  
BEHAVIOR OF THE  $w$  FUNCTIONS FOR  $\lambda \rightarrow 0$  ( $x = z - d_1$ )

term	in $\lambda^2 e^{-\lambda\delta x}$	in $\lambda e^{-\lambda\delta x}$	in $e^{-\lambda\delta x}$
$-w_0^e \lambda$	$-A_j/2$	$-A_j S/2$	$A_j B_j/4 + C_j/2 - A_j S^2/4$
$\delta w_1^e \lambda$	$A_j$	$A_j S$	$-A_j D_j/2 + A_j S^2/2$
$-w_2^e \lambda$	$-A_j/2$	$-A_j S/2$	$A_j B_j/4 - C_j/2 - A_j S^2/4$
$\delta w_0^h \lambda$	0	$F_j/2 + G_j/2$	$F_j S/2 + G_j S/2$
$-w_1^h \lambda$	0	$-G_j$	$-G_j S$
$\delta w_2^h \lambda$	0	$F_j/2 - G_j/2$	$F_j S/2 - G_j S/2$

biological medium, the uppermost layer of the stratified medium consists of lossy material. In that case there are no poles on the real  $\lambda$  axis and the branch point itself is not located on that axis. These considerations lead to the conclusion that part of the integration in (24) can be carried out along the real  $\lambda$  axis. This is similar to the approach used in [3], where it is stated that due to the presence of losses integration along the real axis becomes the most efficient.

### B. Analytical Integration of Part of the Integrals

A first difficulty in the calculation of (24) is the behavior of the integrands  $w_i \lambda$  for  $\lambda \rightarrow \infty$ . To find this behavior we start from

$$\lim_{\lambda \rightarrow \infty} \Gamma = \lim_{\lambda \rightarrow \infty} (\lambda^2 - k^2)^{1/2} = \lambda - k^2/2\lambda. \quad (26)$$

The value of  $k$  was defined by (5). Substituting this limit in the  $\alpha$ 's and  $\beta$ 's given in the Appendix and inserting those values in the expressions for the  $e$ 's and the  $h$ 's, the following final results are obtained: For each layer  $j = 2, \dots, n$  the product  $\lambda w_i(z, \lambda)$ , with  $i = 0, 1, 2$ , in the integrand of (24) decays exponentially with a factor  $\exp[-\lambda(z - d_1)]$  ( $\delta = 1$  in Table I). In the first layer ( $j = 1$ ) this product exhibits an exponential growth with this same factor ( $\delta = -1$  in Table I). For the six different products (subscript 0, 1, or 2 and superscript  $e$  or  $h$ ) the first three terms of the expansion for  $\lambda \rightarrow \infty$  are given in Table I. The coefficients  $A_j$ ,  $B_j$ ,  $C_j$ ,  $D_j$ ,  $F_j$ ,  $G_j$ , and  $S_j$  are given by

$$S_j = [k_j^2(z - d_{j-1}) + k_{j-1}^2(d_{j-1} - d_{j-2}) + \dots + k_2^2(d_2 - d_1)]/2 \\ F_j = (1/2) \sum_{i=2}^j \frac{2\epsilon_i}{\epsilon_i + \epsilon_{i-1}} \quad D_j = \sum_{i=2}^j (k_{i-1}^2 - k_i^2) \frac{\epsilon_{i-1}}{\epsilon_i + \epsilon_{i-1}} \\ G_j = (1/2) \sum_{i=2}^j \frac{2\mu_{i-1}}{\mu_i + \mu_{i-1}} \quad A_j = F_j/(j\omega\epsilon_j) \\ B_j = D_j + k_j^2 \quad C_j = -j\omega\mu_j G_j. \quad (27)$$

These results are valid for  $j = 2, \dots, n$ . If  $j = 1$  we have

$$S_1 = k_1^2(d_1 - z)/2 \\ A_1 = A_2 \quad B_1 = B_2 \quad C_1 = C_2, \\ F_1 = \epsilon_1 F_2/\epsilon_2 \quad D_1 = -\epsilon_2 D_2/\epsilon_1 \quad G_1 = \mu_2 G_2/\mu_1. \quad (28)$$

TABLE II  
CONTRIBUTION TO (24) COMING FROM THE ASYMPTOTIC VALUES  
OF THE INTEGRANDS IN (25) WITH  $x = z - d_1$  AND  
 $\tau = (x^2 + \rho^2)^{-1/2}$

	$i = 0$	$i = 1$	$i = 2$
$m = 0$	$\tau$	$(1 - x\tau)/\rho$	$(1 - x\tau)^2/(\rho^2\tau)$
$m = 1$	$x\tau^3$	$\rho\tau^3$	$[2 - (2x^3 + 3x\rho^2)\tau^3]/\rho^2$
$m = 2$	$(2x^2 - \rho^2)\tau^5$	$3\rho x\tau^5$	$3\rho^2\tau^5$

As the arguments of the Bessel functions  $J_i$  in (24) are real, the results in Table I show that the integrands of (24) have an exponential decay determined by the longitudinal distance ( $z - d_1$ ) between the location of the exciting current and the observation point. This ensures convergence of the integration over  $\lambda$  from 0 to  $\infty$ . However, this is not the case when this distance becomes zero, i.e., in the plane of the exciting current. In that case the integrands become infinite as a power of  $(\lambda)^{3/2}$  for the case of the electric field (superscript  $e$ ) and as a power of  $(\lambda)^{1/2}$  for the case of the magnetic field (superscript  $h$ ). This can easily be checked from Table I in conjunction with the fact that the Bessel functions  $J_i(\lambda\rho)$  have a  $(\lambda\rho)^{-1/2}$  dependence for  $\lambda \rightarrow \infty$  and for a fixed  $\rho$  value. This special case for  $z = d_1$  is very important if the Green's dyadics are to be used as the basis for the solution of an integral equation. The integral of the asymptotic parts given in Table I can be calculated analytically. To that purpose we need the following integrals:

$$\int_0^\infty \lambda^m J_i(\lambda\rho) e^{-\lambda x} d\lambda \quad \text{for } m = 0, 1, 2 \text{ and } i = 0, 1, 2. \quad (29)$$

The notation  $x$  stands for the distance ( $z - d_1$ ). These integrals can be derived from results in the literature [13]. The final results are shown in Table II, where  $\tau = (x^2 + \rho^2)^{-1/2}$ .

Although it would be possible to disregard the cases where ( $z - d_1$ ) differs from zero, we take advantage of the fact that the behavior for  $\lambda \rightarrow \infty$  can be found analytically to reduce the burden on and to enhance the speed of the numerical calculation. Strictly speaking, the integrals in (29) with  $x = 0$  do not exist. However, in the problem we are dealing with we are only interested in the limit  $x \rightarrow 0$ . It is not allowed to interchange the integration and the limiting process. The limits for  $x = 0$  are easily found from Table II. These limits become singular for  $\rho \rightarrow 0$ . As for  $x \rightarrow 0$ , this is also important when using the Green's dyadics as the kernel of an integral equation if source and observation point coincide. This difficulty is one of the reasons why the authors in [6] state that they abandoned the use of the above Green's dyadics for their purpose. It is shown in another paper [7] that this difficulty can be circumvented, keeping the advantage of the Green's function approach presented here.

#### C. Numerical Calculation of the Remaining Fourier-Bessel Integrals

If we subtract the parts shown in Table II from the integrands in (24) and determine the integral of the sub-

tracted parts in the way discussed above, we only need to calculate integrals of the form

$$\int_0^\infty f(x, \lambda) J_i(\lambda\rho) e^{-\lambda x} d\lambda \quad \text{for } i = 0, 1, 2 \quad (30)$$

where  $x = z - d_1$  and  $f(x, \lambda) = 0(1/\lambda)$  for  $\lambda \rightarrow \infty$ . As long as  $\rho \neq 0$  the integral in (30) is convergent, even for  $x = 0$ . In this last case, the absolute value of the integrand decays as  $1/\lambda^{3/2}$ . If, however,  $\rho = 0$ , the integral in (30) becomes zero for  $i = 1, 2$  but difficulties can be expected for  $i = 0$  and  $x = 0$ . In that last case the  $1/\lambda$  behavior of  $f(x = 0, \lambda)$  no longer suffices to make the integral convergent. Two types of such integrals have to be considered. A first integral is derived from  $W_0^e$  in (24). In that case one can rather easily prove that  $f(x = 0, \lambda) = 0(1/\lambda^2)$  for  $\lambda \rightarrow \infty$ . A second integral, however, is derived from  $W_0^h$  and the integral is divergent for  $\rho = 0$  and  $x = 0$ . To deal with this difficulty we could follow an approach similar to the one adopted in the previous section. As our interest is more focused on the calculation of the electric Green's dyadic as the basis for the solution of an electric field integral equation, we will not go into further details here. Working with lossy media, neither a branch point nor poles are located on the real  $\lambda$  axis. For the actual numerical integration we subdivide the integration interval into two parts:

$$\int_0^{\lambda_c} f(x, \lambda) J_i(\lambda\rho) e^{-\lambda x} d\lambda + \int_{\lambda_c}^\infty f(x, \lambda) J_i(\lambda\rho) e^{-\lambda x} d\lambda. \quad (31)$$

The upper limit  $\lambda_c$  is chosen such that both  $f(x, \lambda)$  and  $J_i(\lambda\rho)$  take their asymptotic form for  $\lambda \rightarrow \infty$ . The first integral in (31) can be rewritten as

$$\int_0^\infty g(x, \lambda) J_i(\lambda\rho) d\lambda \quad \text{for } i = 0, 1, 2. \quad (32)$$

This integral is calculated using a Romberg extrapolation scheme. For the integrals under consideration this scheme proved to be a very efficient one.

Finally, the second integral in (31) must be calculated. To this end we introduce  $\lambda\rho$  as a new integration variable, rewrite the Bessel function  $J_i(\lambda\rho)$  as  $[H_i^{(2)}(\lambda\rho) + H_i^{(1)}(\lambda\rho)]/2$ , and introduce the asymptotic form for large arguments of the Hankel functions:

$$\begin{aligned} H_i^{(1)}(z) &= [P_i(z) + jQ_i(z)] e^{j(z-\alpha)} \\ H_i^{(2)}(z) &= [P_i(z) - jQ_i(z)] e^{-j(z-\alpha)} \end{aligned} \quad (33)$$

with

$$\alpha = (2i+1)(\pi/4)$$

$$P_i(z) = (2/\pi z)^{1/2} [1 - c_1/z^2 + c_2/z^4 + \dots]$$

$$Q_i(z) = (2/\pi z)^{1/2} [d_1/z - d_2/z^3 + \dots]. \quad (34)$$

The constants  $c_1, c_2, \dots$  and  $d_1, d_2, \dots$  are to be found in the literature [13]. The integral to be calculated takes the

form

$$(1/2\rho)e^{-j\alpha}\int_{\lambda_c\rho}^{\infty}f(z, \lambda)[P_i(\lambda\rho) + jQ_i(\lambda\rho)]e^{-\beta^{(1)}(\lambda\rho)}\rho d\lambda \\ + (1/2\rho)e^{+j\alpha}\int_{\lambda_c\rho}^{\infty}f(z, \lambda) \\ \cdot [P_i(\lambda\rho) - jQ_i(\lambda\rho)]e^{-\beta^{(2)}(\lambda\rho)}\rho d\lambda \quad (35)$$

where  $\beta^{(1)} = x/\rho - j$  and  $\beta^{(2)} = x/\rho + j$ . For the first integral in (35) we change the integration path from the real axis to the line  $\lambda\rho = t/\beta^{(1)} + \lambda_c\rho$ , with  $0 \leq t < \infty$ . The value of  $\lambda_c$  can be chosen such that no pole or branch cut contributions need be taken into account by the change of integration path. A similar reasoning can be applied to the second integral in (35). For that integral we change the integration path to  $\lambda\rho = t/\beta^{(2)} + \lambda_c\rho$ . Both integrals can be taken together. The final result is

$$(1/2\rho)\int_0^{\infty}g(t)e^{-t}dt \quad (36)$$

where  $g(t)$  takes the form

$$\exp[-(\beta^{(1)}\lambda_c\rho + j\alpha)]f[z, \lambda^{(1)}] \\ \cdot \{P_i[\lambda^{(1)}\rho] + jQ_i[\lambda^{(1)}\rho]\}/\beta^{(1)} \\ + \exp[-(\beta^{(2)}\lambda_c\rho - j\alpha)]f[z, \lambda^{(2)}] \\ \cdot \{P_i[\lambda^{(2)}\rho] - jQ_i[\lambda^{(2)}\rho]\}/\beta^{(2)} \quad (37)$$

and with  $\lambda^{(1)} = t/\beta^{(1)}\rho + \lambda_c$  and  $\lambda^{(2)} = t/\beta^{(2)}\rho + \lambda_c$ . The integral (36) can now be evaluated in a numerically accurate fashion by applying Gauss-Laguerre quadrature formulas.

## V. CONCLUSIONS

We have shown in this paper that the determination of the electric and magnetic fields everywhere in space generated by a surface current density located at the interface of a planar stratified medium reduces essentially to the calculation of Fourier-Bessel integrals. Although this result is quite familiar, great effort was spent to formulate the problem in such a way that numerical difficulties in the calculation of those Fourier-Bessel integrals can be circumvented. The analytical procedures introduced for that purpose make it possible to calculate the Green's dyadics in the source region itself and in the presence of media with high losses. This is an essential step towards the use of these dyadics in the formulation of an integral equation for the surface current on a microstrip antenna. It is shown elsewhere [7] that such an integral equation based on the dyadics calculated in the present paper leads to the solution of the power deposition of a microstrip antenna inside a layered biological tissue.

## APPENDIX SOLUTION OF THE TRANSMISSION LINE PROBLEM FOR THE $\alpha$ 's AND $\beta$ 's

We will not go into the details of the calculations. The final result is

$$\alpha_1 = -T_1 e^{-\Gamma_1 d_1} \frac{[k_2][M_{nn-1}]\cdots[M_{32}][N_2]}{[k_2][M_{nn-1}]\cdots[M_{21}][k_1]} \\ \alpha_n = -T_n(1 - e^{-2\Gamma_1 d_1}) \frac{e^{\Gamma_n d_{n-1} - \Gamma_{n-1}(d_{n-1} - d_{n-2}) - \cdots - \Gamma_2(d_2 - d_1)}}{[k_2][M_{nn-1}]\cdots[M_{21}][k_1]} \\ [c_j] = -T_j(1 - e^{-2\Gamma_1 d_1}) e^{\Gamma_j d_{j-1} - \Gamma_{j-1}(d_{j-1} - d_{j-2}) - \cdots - \Gamma_2(d_2 - d_1)} \\ \cdot \frac{[M_{jj+1}]\cdots[M_{n-1n}][k_n]}{[k_2][M_{nn-1}]\cdots[M_{21}][k_1]} \quad (A1)$$

with  $[c_j] = \begin{vmatrix} \alpha_j \\ \beta_j e^{2\Gamma_j d_j} \end{vmatrix}$ .

In (A1)  $j$  takes the values 2 to  $n-1$ . For  $T_1$ ,  $T_j$ , and  $T_n$  we have

$$T_1 = 1/(Y_1'Y_2') \quad T_j = 1/(2Y_j'Y_{j-1}'\cdots Y_1') \\ T_n = 1/(2Y_n'Y_{n-1}'\cdots Y_1'). \quad (A2)$$

In each layer the quantity  $Y' = j\omega\epsilon/\Gamma$ . The matrices  $[M'_{jj+1}]$  and  $[M'_{j+1j}]$  are defined as

$$[M'_{jj+1}] = (1/2) \begin{vmatrix} (m'+n') & (m'-n')e^{2\Gamma_{j+1}d_j} \\ (m'-n')e^{-2\Gamma_j d_j} & (m'+n')e^{2(\Gamma_{j+1}-\Gamma_j)d_j} \end{vmatrix} \quad (A3)$$

and

$$[M'_{j+1j}] \\ = (1/2) \begin{vmatrix} (m'+n')e^{-2(\Gamma_j-\Gamma_{j+1})d_j} & (n'-m')e^{2\Gamma_{j+1}d_j} \\ (n'-m')e^{-2\Gamma_j d_j} & (m'+n') \end{vmatrix} \quad (A4)$$

where  $m' = 1/Y'_{j+1}$  and  $n' = 1/Y'_j$ . We have also introduced the matrices  $[c_j]$ ,  $j = 1, \dots, n$ ,  $[N]$ ,  $[k_1]$ ,  $[k_2]$  and  $[k_n]$ :

$$[c_j] = \begin{vmatrix} \alpha_j \\ \beta_j \end{vmatrix} \quad [N] = \begin{vmatrix} 1/2e^{2\Gamma_2 d_1} \\ -1/2 \end{vmatrix} \\ [k_1] = \begin{vmatrix} 1 \\ -1 \end{vmatrix} \quad [k_2] = \begin{vmatrix} 0 & 1 \end{vmatrix} \quad [k_n] = \begin{vmatrix} 1 \\ 0 \end{vmatrix}. \quad (A5)$$

The results in (A2), (A3), and (A4) show that only divisions by  $Y'$  occur. As  $Y' = j\omega\epsilon/\Gamma$  no difficulty occurs when  $\Gamma$  becomes zero. Analogous results are found for the double-primed quantities. In that case  $T_1$ ,  $T_j$ , and  $T_n$  become

$$T_1 = 1 \quad T_j = (Y_{j-1}''Y_{j-2}''\cdots Y_2'')/2 \\ T_n = (Y_{n-1}''Y_{n-2}''\cdots Y_2'')/2. \quad (A6)$$

The matrices  $[M''_{jj+1}]$  and  $[M''_{j+1j}]$  are defined in the same way as their single-primed counterparts in (A3) and (A4),

but  $m'$  must be replaced by  $m'' = Y_j''$  and  $n'$  must be replaced by  $n'' = Y_{j+1}''$ . Note that now only products by  $Y''$  occur. As  $Y'' = -\Gamma/j\omega\mu$  no difficulty occurs when  $\Gamma$  becomes zero. Remember that  $\beta_n = 0$  and  $\beta_1 = -\alpha_1$  for both single- and double-primed quantities.

Finally we show that only decaying exponentials play a role in the matrix products occurring in (A1). We first look at the denominator of the  $\alpha$ 's and  $\beta$ 's. We also need the following general result:

$$\begin{vmatrix} B_1 e^{-2\Gamma_{j+1}d_{j+1}} & B_2 \\ A_{11} e^{-2(\Gamma_j - \Gamma_{j+1})d_j} & A_{12} e^{2\Gamma_{j+1}d_j} \\ A_{21} e^{-2\Gamma_j d_j} & A_{22} \end{vmatrix} = \begin{vmatrix} C_1 e^{-2\Gamma_j d_j} & C_2 \end{vmatrix} \quad (A7)$$

where

$$\begin{aligned} C_1 &= B_1 A_{11} e^{-2\Gamma_{j+1}(d_{j+1} - d_j)} + B_2 A_{21} \\ C_2 &= B_1 A_{12} e^{-2\Gamma_{j+1}(d_{j+1} - d_j)} + B_2 A_{22}. \end{aligned} \quad (A8)$$

Only decaying exponentials are involved in the calculation of  $C_1$  and  $C_2$ . The denominator in (A1) is calculated starting from  $[k_2]$ . Multiplication with  $[M_{nn-1}]$  gives a row matrix of the form of the  $B$  matrix on the left-hand side of (A7).  $[M_{n-1n-2}]$  is of the form of the  $A$  matrix in (A7). Hence, multiplication results in the  $C$  matrix, which has the same form as the  $B$  matrix. The above process is repeated at every step of the denominator calculation. Analogous reasoning applies to the numerator of  $\alpha_1$ . For the calculation of the numerator of  $[c_j]$  we start from  $[k_n]$ . The stability of the procedure can be proved using different  $A$ ,  $B$ , and  $C$  matrices:

$$\begin{vmatrix} C_1 \\ C_2 e^{-2\Gamma_j d_j} \end{vmatrix} = \begin{vmatrix} A_{11} & A_{12} e^{2\Gamma_{j+1}d_j} \\ A_{21} e^{-2\Gamma_j d_j} & A_{22} e^{2(\Gamma_{j+1} - \Gamma_j)d_j} \end{vmatrix} \begin{vmatrix} B_1 \\ B_2 e^{-2\Gamma_{j+1}d_{j+1}} \end{vmatrix} \quad (A9)$$

where

$$\begin{aligned} C_1 &= B_2 A_{12} e^{-2\Gamma_{j+1}(d_{j+1} - d_j)} + B_1 A_{11} \\ C_2 &= B_2 A_{22} e^{-2\Gamma_{j+1}(d_{j+1} - d_j)} + B_1 A_{21}. \end{aligned} \quad (A10)$$

#### ACKNOWLEDGMENT

The authors would like to thank the reviewers for their comments, which substantially enhanced the quality of the presentation of the paper.

#### REFERENCES

- [1] T. Sphicopoulos, V. Theodoris, and F. Gardiol, "Dyadic Green function for the electromagnetic field in multilayered isotropic media: an operator approach," *Proc. Inst. Elec. Eng.*, vol. 132, pt.H, no. 5, pp. 329-334, Aug. 1985.
- [2] J. Wang, "General method for the computation of radiation in stratified media," *Proc. Inst. Elec. Eng.*, vol. 132, pt.H, no. 1, pp. 58-62, Feb. 1985.
- [3] J. Mosig and T. Sarkar, "Comparison of quasi-static and exact electromagnetic fields from a horizontal electric dipole above a lossy dielectric backed by an imperfect ground plane," *IEEE Trans. Microwave Theory Tech.*, vol. MTT-34, pp. 379-387, Apr. 1986.
- [4] T. Itoh and W. Menzel, "A full-wave analysis method for open microstrip structures," *IEEE Trans. Antennas Propagat.*, vol. AP-29, pp. 63-67, Jan. 1981.
- [5] B. Roudot, C. Terret, and J. P. Daniel, "Fundamental surface-wave effects on microstrip antenna radiation," *Electron. Lett.*, vol. 21, no. 23, pp. 1112-1113, Nov. 1985.
- [6] J. Mosig and F. Gardiol, "General integral equation formulation for microstrip antennas and scatterers," *Proc. Inst. Elec. Eng.*, vol. 132, pt.H, no. 7, pp. 424-432, Dec. 1985.
- [7] L. Beyne and D. De Zutter, "Power deposition of a microstrip applicator radiating into a layered biological structure," *IEEE Trans. Microwave Theory Tech.*, vol. 36, pp. 126-131, Jan. 1988.
- [8] J. A. Kong, "Electromagnetic fields due to dipole antennas over stratified anisotropic media," *Geophysics*, vol. 37, no. 6, pp. 958-966, Dec. 1975.
- [9] S. M. Ali and S. F. Mahmoud, "Electromagnetic fields of buried sources in stratified anisotropic media," *IEEE Trans. Antennas Propagat.*, vol. AP-27, no. 5, pp. 671-678, Sept. 1979.
- [10] C. Tang, "Electromagnetic fields due to dipole antennas embedded in stratified anisotropic media," *IEEE Trans. Antennas Propagat.*, vol. AP-27, no. 5, pp. 665-670, Sept. 1979.
- [11] B. Bhat and S. Koul, "Lumped capacitance, open-circuit end effects and edge-capacitance of microstrip-like transmission lines for microwave and millimeter-wave applications," *IEEE Trans. Microwave Theory Tech.*, vol. MTT-32, pp. 433-439, Apr. 1984.
- [12] N. Marcuvitz and L. Felsen, *Radiation and Scattering of Waves*. Englewood Cliffs, NJ: Prentice-Hall, 1973, ch. 5.
- [13] W. Magnus, F. Oberhettinger, and R. Soni, *Formulas and Theorems for the Special Functions of Mathematical Physics*, 3rd ed. New York: Springer-Verlag, 1966.

†

**Luc Beyne** was born in Ostend, Belgium, on July 1, 1963. He received the degree of electrical engineer (a five-year program equivalent to the M.S. degree) from the University of Ghent, Belgium, in 1986. At present he is with Alcatel Bell Telephone, Antwerp, Belgium, where he is engaged in broad-band ISDN research.



†

**Daniel De Zutter** was born in Eeklo, Belgium, on November 8, 1953. He received the degree of electrical engineer (a five-year program equivalent to the M.S. degree) from the University of Ghent, Belgium, in 1976. From September 1976 to September 1984, he was a research and teaching assistant at the Laboratory of Electromagnetism and Acoustics of the University of Ghent. In October 1981 he obtained the Ph.D. degree from the same university and in April 1984 he completed a thesis leading to the "Aggregaat van het Hoger Onderwijs," a degree equivalent to the German "Habilitation" and the French "Agrégation."



Most of his scientific work up to 1984 dealt with the electrodynamics of moving media. In October 1984 he became a Research Associate with the National Fund for Scientific Research of Belgium. He is now engaged in hyperthermia research and in research on high-frequency microstrip interconnections.